



AN EXPERIMENTAL STUDY OF REGULAR LONG CRESTED WAVES OVER A CRESCENT TYPE SHOAL

Wen-Kai Weng

*Department of Harbor and River Engineering, National Taiwan Ocean University, Keelung, Taiwan, R.O.C.,
wkweng@mail.ntou.edu.tw*

Jaw-Guei Lin

Department of Harbor and River Engineering, National Taiwan Ocean University, Keelung, Taiwan, R.O.C.

Chun-Sien Hsiao

Department of Harbor and River Engineering, National Taiwan Ocean University, Keelung, Taiwan, R.O.C.

Follow this and additional works at: <https://jmstt.ntou.edu.tw/journal>



Part of the [Ocean Engineering Commons](#)

Recommended Citation

Weng, Wen-Kai; Lin, Jaw-Guei; and Hsiao, Chun-Sien (2013) "AN EXPERIMENTAL STUDY OF REGULAR LONG CRESTED WAVES OVER A CRESCENT TYPE SHOAL," *Journal of Marine Science and Technology*. Vol. 21: Iss. 2, Article 15.

DOI: 10.6119/JMST-013-0313-1

Available at: <https://jmstt.ntou.edu.tw/journal/vol21/iss2/15>

This Research Article is brought to you for free and open access by Journal of Marine Science and Technology. It has been accepted for inclusion in Journal of Marine Science and Technology by an authorized editor of Journal of Marine Science and Technology.

AN EXPERIMENTAL STUDY OF REGULAR LONG CRESTED WAVES OVER A CRESCENT TYPE SHOAL

Wen-Kai Weng, Jaw-Guei Lin, and Chun-Sien Hsiao

Key words: regular waves, crescent shoal, wave energy.

ABSTRACT

Converting the ocean wave energy into electric power is one possibility of the development of alternative and non-polluting sources of energy. Many researches concerning converters and their converting efficiency of wave power were developed and discussed in the last years. However, converting wave energy into electric power does not only depend upon converting system but condition of sea state essentially. A calm sea state with lower wave energy is difficult to drive converting device working and is unable to satisfy the minimum economical requirement. Unfortunately, wave heights in the sea state around Taiwan are mostly too smaller to extract the wave energy except winter and typhoon. In this study, a crescent type shoal was created for concentrating wave energy and enhancing energy density. The new submerged artificial topography is constructed as convex topography at seaside with increasing slope to the crest line and decreasing slope to the concave shape topography at landside. A series of hydraulic model tests in a wave basin about the transformations and deformations of regular long crested waves over this type shoal had been accomplished in order to evaluate its efficiency on collecting wave energy. The results show the crescent type shoal can concentrate wave energy and enlarge energy density behind the shoal, and all the experimental results indicate wave energy ratio above 8 times of the incident wave energy can be obtained for incoming wave passing through the shoal, especially for the case of wave period $T = 1.5$ sec this ratio reaches to 14 times.

I. INTRODUCTION

When planning a wave power plant at a site, the efficiency, sustainability and stability of wave energy are always the

major concerns in the feasibility study. Wave heights, wave periods and the demand of electricity in different season were evaluated. For most coastal area around Taiwan, the ocean waves can be roughly classified into three seasons: summer monsoon wind season (mostly southwest winds), winter monsoon wind season (mostly northeast winds) and typhoon wind season. Except for the extreme wave heights during typhoon season intrusions, only the winter monsoon season fits the goal that the wave height is higher than 5 meters, and wave heights are mostly below 1 meter in other days which is not good for the wave energy extraction. The demand of electricity in Taiwan, however, on the other hand encounters its highest requirement in the summer season. This means that the period of supply of wave energy and the period of demand of electricity are inconsistent. How to concentrate the wave energy in the moderate wave season becomes a major topic in the use of wave energy in Taiwan.

From the wave theories, the dynamic energy of a wave is proportional to the square of the wave height and to the wave period of the motion. The wave energy is usually expressed as $E = \rho g H^2 L / 8$, the wave energy flux is written as $\bar{E} = E / L = \rho g H^2 / 8$ and the wave power is $\bar{P} = \bar{E} C_g$, where ρ is water density, g is the gravitational acceleration, H is the wave height, L is the wave length, and C_g is the group velocity of the wave. Some parameters were also proposed to evaluate the potential wave energy, for example, by referring to the sea state parameter records from the Coquille River CDIP 0037 buoy, EPSI [6] defined an estimation of the incident wave power J which equals to the wave energy flux across a vertical plane (in kW/m), i.e. $J = 0.42 H_S^2 T_p$, where the multiplier 0.42 in the above equation is exact for any sea state that is well represented by a two-parameter Bretschneider spectrum, but could range from 0.3 to 0.5, depending on the relative amounts of energy in sea and swell components and the exact shape of the wave spectrum, H_S is the significant wave height (in m) and T_p is the peak wave period (in sec).

In the nearshore zone, enhancing wave energy density and concentrating wave energy can be obtained from waves shoaling, refraction and diffraction on some specific topog-

Paper submitted 04/03/12; revised 08/31/12; accepted 03/13/13. Author for correspondence: Wen-Kai Weng (e-mail: wkweng@mail.ntou.edu.tw).
Department of Harbor and River Engineering, National Taiwan Ocean University, Keelung, Taiwan, R.O.C.

raphy, but the specific topography may also result in dissipation of energy due to the frictional loss of seabed bottom and wave breaking. This study is aimed at creating a submerged artificial topography which can concentrate the nearshore wave energy and enlarge the wave height behind the structure for the purpose of effective extraction of wave energy.

For studies on wave behavior around a submerged shoal, several researches have worked on a circular and elliptic shoal, such as Berkhoff *et al.* [1, 2] who first derived a 2D elliptic type mild slope equation from the linear wave theory to analyze the wave refraction/diffraction problem, and they also simulated the wave field numerically around an elliptic shoal with major axis of 8 m and minor axis of 6 m seated on a 1/50 slope bottom to evaluate the refraction and diffraction of linear long crested waves behind the shoal, and proved the waves can concentrate behind the shoal. The results also were compared with hydraulic model test results with good consistency. Kirby and Dalrymple [11] simulated the weak non-linear/linear waves passing through an elliptic shoal numerically using the parabolic type mild slope equation, and they also compared the numerical results with experimental data from the hydraulic model test. Ebersole [4] numerically simulated the deformation of linear waves passing through a semi-circular shoal or an elliptic shoal by using the finite difference method, the results were compared with hydraulic model test results. And the final result in this literature had been applied in practice at Oregon Inlet, North Carolina, USA. Panchang *et al.* [15] have solved the wave refraction-diffraction problem around a circular shoal seated on constant water depth sea bottom and on constant slope sea bottom using the mild slope equation. Hsu *et al.* [6] used the elliptic mild slope equation and finite element method to simulate wave refraction, diffraction and reflection problem. All these studies, however, focused on wave refraction and diffraction problem around a shoal and the development of numerical technique, and some of them do not consider the wave reflection or wave nonlinearity phenomena.

By using the hydraulic model tests of wave refraction/diffraction of regular/irregular waves around an elliptic shoal with major axis of 8 m and minor axis of 6m seated on a 1/40 slope bottom, and taking the overall wave field measurements, Wu [16] and Huang [7] discussed the variations of wave energy around the shoal. The shoal was found can gathering the wave energy into a small region behind the shoal. In stead of a circular/elliptic shoal, this study will further study the distribution of wave energy due to the wave shoaling, refraction and diffraction around a crescent shoal.

For the studies about the wave energy gathering function of a crescent structure, only a few researches were presented. Kudo *et al.* [12, 13] evaluated the wave energy gathering function of a submerged convex topography or a submerged horizontal crescent plate via hydraulic model tests and numerical simulations with boundary element method. The results showed that the wave energy can be piled up behind the structures. The values of experimental results are found



Fig. 1. “Jiao”, a device used in the Chinese divination.

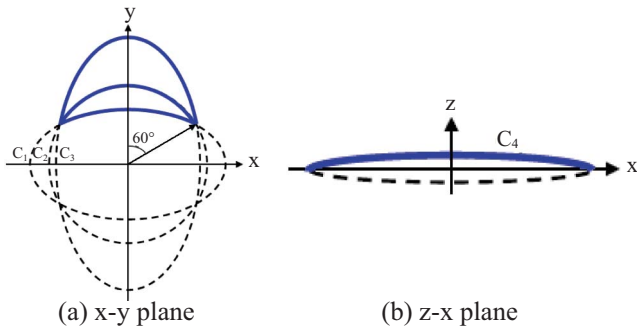
to be greater than numerical results which might be induced by the wave shoaling, nonlinear wave interaction and wave breaking effects. Imai *et al.* [8-10] focused their studies on wave gathering effect of a submerged horizontal crescent plate. The wave forces above and under the horizontal plate were firstly observed, and an incline plate was deployed behind the plate to observe the wave amplification. The results showed that the installation of submerged horizontal crescent plate can increase the efficiency of wave power gathering device. Other tests were also done by dividing the floating plate into several parts anchored with tension cable. The wave gathering efficiency and influences of cable tension force on wave heights were evaluated and confirmed. Mei [14] analyzed an array of small buoys in well-separated rows parallel to a coast, and compared its efficiency with that of a large buoy of equal volume.

Following the concepts and the experiences from previous studies, this study designed a new type of submerged crescent shoal by referring to the Chinese traditional divination tool “Jiao” as shown in Fig. 1. The shoal has crescent shape in horizontal projection with convex side facing to offshore which is composed by two elliptic curves, the crest line of the shoal is form by a circle horizontally and a parabolic curve vertically to create its contour. With this topography, the transformation of water waves passing through the submerged shoal is assumed to act similarly as the rays of light passing through a convex mirror which may produce the light focusing effect. This study evaluated the wave concentration effects around such topography induced by regular waves via hydraulic model tests, under the condition of non-breaking of the waves. The wave height distributions and their directional spreading were measured and evaluated.

In the following paragraphs, the experimental setup and the facilities of the hydraulic model tests will be firstly introduced. The analyses and evaluation of the experimental results then will be followed.

II. LAYOUT OF NEW CRESCENT TYPE SHOAL

The horizontal projection of the new crescent shoal is formed by the intersection of two elliptic curves with different



Elliptic Circle	Radius
C ₁	$R_x = 6.19 \text{ m}, R_y = 3.5 \text{ m}$
C ₂	$R_x = 5 \text{ m}, R_y = 5 \text{ m}$
C ₃	$R_x = 4.56 \text{ m}, R_y = 8 \text{ m}$
C ₄	$R_x = 4.33 \text{ m}, R_z = 0.4 \text{ m}$

Fig. 2. Geometrical composition of the crescent shoal.

axes. As shown in Fig. 2, the radius of major axis (R_x) and minor axis (R_y) are 8 m and 4.56 m, respectively, for outer curve, and 6.19 m and 3.5 m, respectively, for inner curves. The curve of crest line of the shoal is created by a circular curve with 5 m radius. Three curves are designed to have the same center point, and intersect at the same two end points. The angle spanned by two lines formed from these points (one line connects the center and one of the intersection end point and the other line connects the center and the other intersection end point) is 120 degrees. The shoal is designed with its convex side facing to the offshore. Fig. 3 shows the contours and 3D view of the crescent shoal. The elevation of the crest line is generated by an elliptic curve with radius of major axis (R_x) is 4.33 m and radius of minor axis (R_z) is 0.4 m, the highest elevation of the shoal is thus 0.4 m at the middle of the crest line. The topography of the front side changes smoothly and mildly, but the topography of the rare side changes steeply and rapidly. The highest point of the shoal appears at the middle of the crest line and then the crest line declines to the two ends. Due to the shoaling, refraction, diffraction effects, when the waves passing through the shoal, shoaling effect enlarges the wave heights and the refraction and diffraction effects changes the wave propagation directions toward the focal point of the curves. Such phenomenon might concentrate and enlarge the wave energy at a specific location behind the shoal, and cause the wave energy become useful.

III. EXPERIMENTAL SETUP

The experiments were carried out at the wave basin in the Ocean Engineering Laboratory of the Department of Harbor and River Engineering, National Taiwan Ocean University. The basin is 50 m long and 50 m wide, and equipped

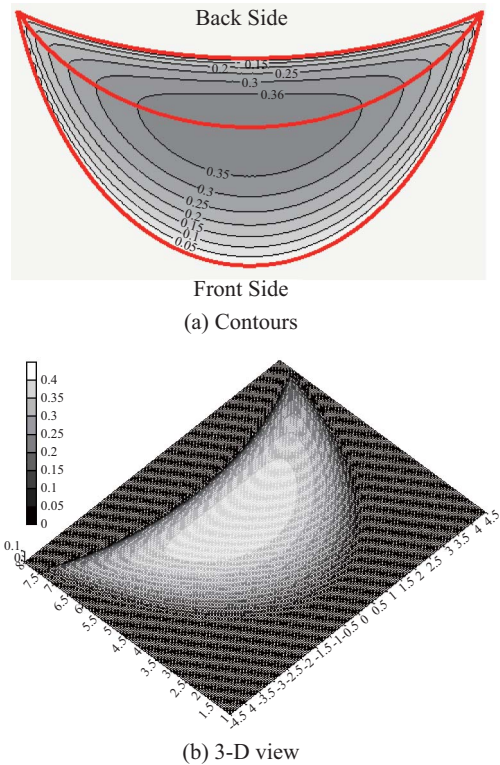


Fig. 3. Contours and 3-D view of the crescent shoal.

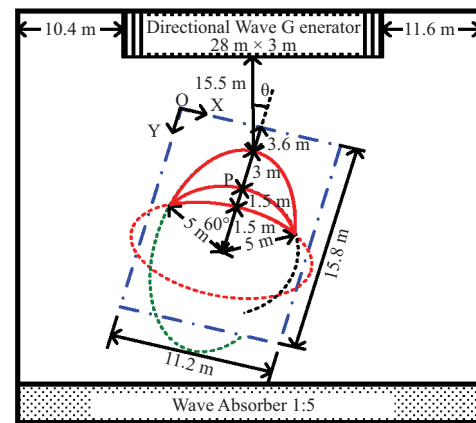


Fig. 4. Layout of the hydraulic experiments.

with a 28 m wide directional irregular wave generator with 56 sets of wave paddles. The crescent shoal model was allocated 18 m away from the center line of the wave generator with an oblique angle of 15 degrees, as shown in Fig. 4. The testing water depth is 0.5 m deep which means the shoal is submerged 0.1 m below the free surface. Except for measuring the variations of water elevations by capacitance wave gauges with 0.4 m interval between each two adjacent testing points, Fig. 5 shows the deployment of testing points and the seven star array wave gauge systems were also deployed to measure the directional characteristics of waves on and behind the shoal. Fig. 6 shows the layout of a start array, and

Table 1. Wave conditions for normal incident regular wave tests.

Wave Period, T (sec)	1.25	1.50	1.75
Wave height, H (cm)	2.40	2.10	2.07
Wave Length, L (m)	2.18	2.83	3.45

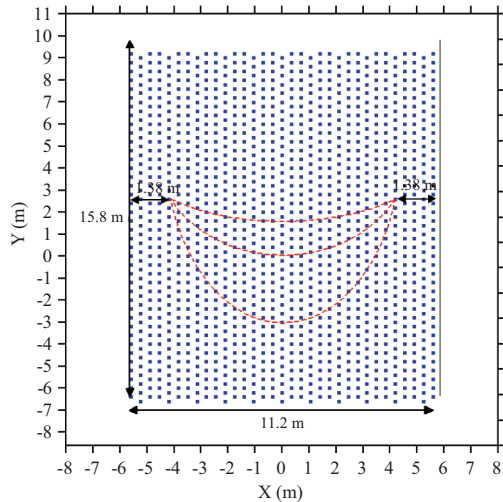


Fig. 5. Distribution of testing points.

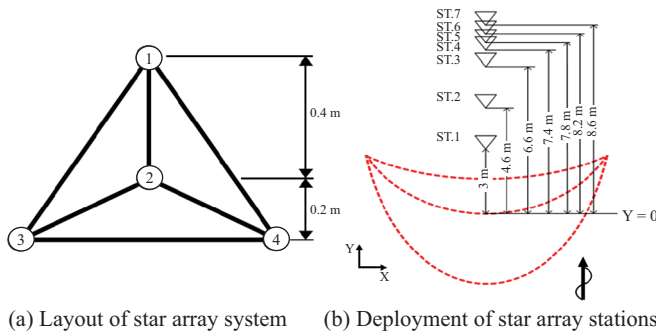


Fig. 6. Measurement of wave directional spreading.

the locations of the seven star arrays of the wave stations. All the experiments were carried out under the circumstance of non-breaking waves.

Table 1 shows the incident wave conditions, wave periods, wave heights and wave lengths at 0.5 m water depth. The experimental results discussed in this paper are categorized into the normal incident wave conditions (i.e. $\theta_i = 0^\circ$). In order to keep the waves non-breaking in any place around the shoal, the wave heights were selected between 2 cm and 3 cm. Each wave condition was tested with 5 cycles. The time series of water elevation at each node was analyzed by zero-up-crossing method to find their representative wave height and period, and by the fast Fourier transform (FFT) to find the spectrum. The time series of four wave gauges in each star

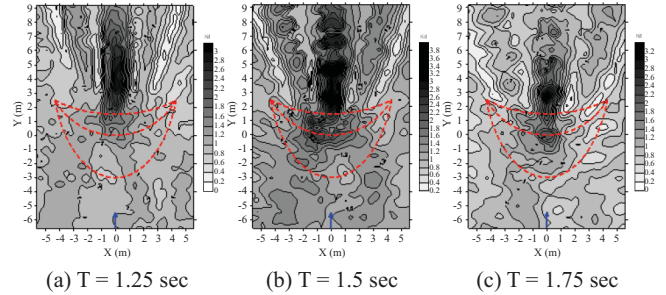


Fig. 7. Non-dimensional wave height distribution around the shoal ($\theta_i = 0^\circ$).

array was analyzed by the theory proposed by Borgman *et al.* [3] in 1969 to find the directional spreading of the wave energy, i.e. the directional spectrum at each star array station.

IV. EXPERIMENTAL RESULTS

Fig. 7 shows the non-dimensional wave height distributions around the shoal with respect to the incident wave height for normal incident wave ($\theta_i = 0^\circ$) with the wave periods of 1.25 sec, 1.5 sec and 1.75 sec respectively. Wave height concentration effects can be found behind the shoal. Following the incident wave direction, the non-dimensional wave height at a certain region is greater than 2.0, and two branches at each side of the center line have wave heights greater than 1.0. The results show that the crescent shoal can concentrate and enlarge the wave energy at some specific location. When observing the results of different wave period, for the long period waves the wave energy is enhanced by the shoal earlier than that for the short period waves following the strength of wave shoaling, refraction and diffraction effects. The highest wave energy pile-up occurs between the top of the crest line of the shoal and the center point. Due to the superposition of refraction waves and diffractions with different directions and phases, the wave heights behind the shoal become alternatively higher and lower than incident wave height, and the non-linearity effect becomes strong.

Fig. 8 shows the variations of water elevation of incident waves (dotted line, $T = 1.5$ sec, located at Y4 position as shown in Fig. 9) and that of refracted/diffracted waves behind the shoal (solid line), and the results show the strong non-linearity behind the shoal. We may see that the component waves with multiple frequencies occur after the regular waves passing through the shoal.

In order to see the variations of the wave energy and frequency before and behind the shoal, Fig. 10 shows spectra at different locations along the center line of the shoal for the cases of incident wave periods are 1.25 sec, 1.5 sec and 1.75 sec, respectively. In each figure, there are five wave spectra for wave gauges located at, along the center line of the shoal, the front end of the shoal (Y1), the top of the crest line (Y2), and the wave gauges with 3.0 m, 4.2 m, and 5.4 m, respectively, (Y3~Y5) away from the crest of the shoal, as

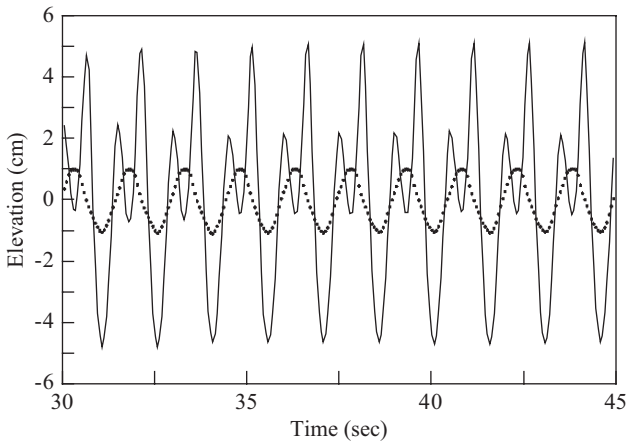


Fig. 8. Variations of water elevations of incident waves and waves behind the shoal. (dotted line: incident waves, solid line: refracted/diffracted waves)

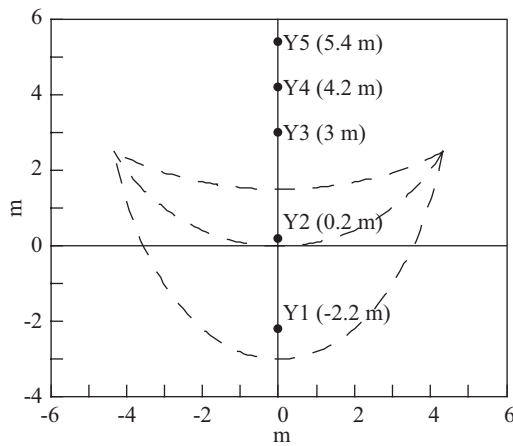
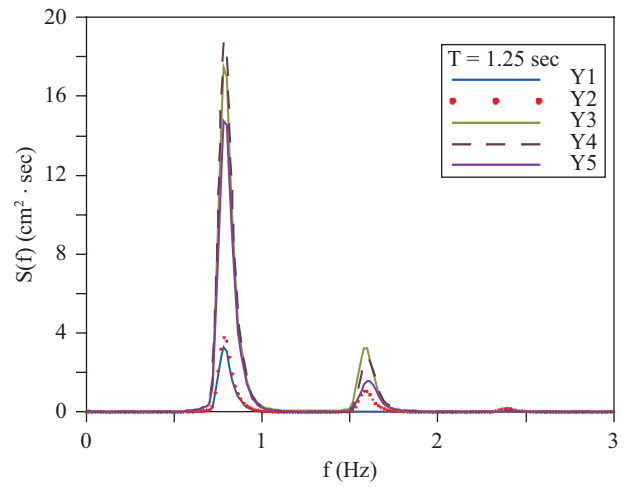


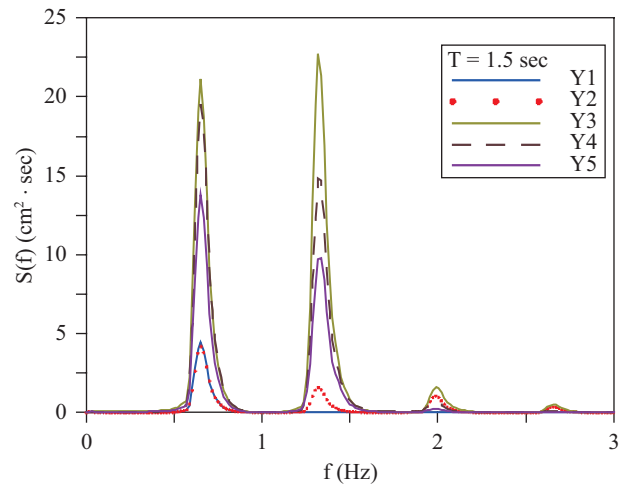
Fig. 9. Wave gauges at various locations (Y1~Y5).

shown in Fig. 9. One may see that when the waves just reach the front end of the shoal, due to the waves traveling on horizontal constant depth bottom, there is only one component wave with peak frequency exist (namely, principle component) in the spectra for all cases. When the waves climb up to the crest line of the shoal and passing through the shoal, the component waves with multiple times of peak frequency exist (namely, the second, third, fourth and fifth components).

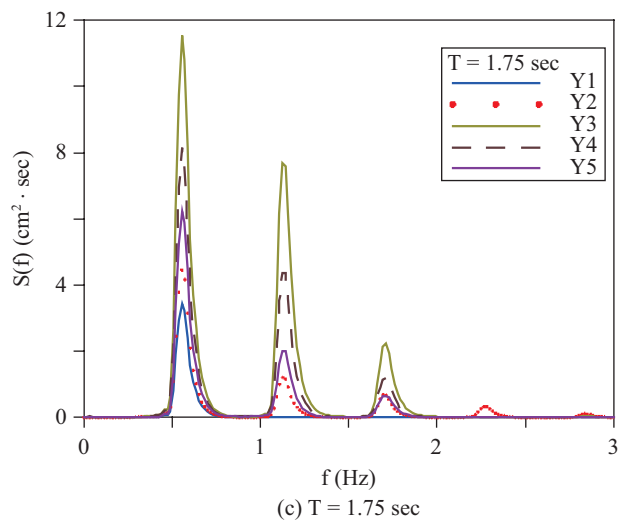
Fig. 10(a) show the spectra for $T = 1.25$ sec case. One may find that the spectrum of waves (Y1) reaching the shoal contains only one component wave with principle wave frequency. The component waves with multiple frequencies occur (Y2) as waves reach to the top of the crest line of the shoal and they should be induced by the wave shoaling effect. After the waves passing through the shoal, however, the spectral density of principle frequency becomes the largest at location Y3, and decreases from location Y4 to Y5 but it still are larger than the waves at the front side of the shoal. The ratio of spectral density is around 4 to 1 between the principle and the second components. The third component



(a) $T = 1.25$ sec



(b) $T = 1.5$ sec



(c) $T = 1.75$ sec

Fig. 10. Wave spectra at various locations ($\theta_i = 0^\circ$).

contains only negligible energy. Fig. 10(b) shows the results for $T = 1.5$ sec case. After the waves pass through the shoal, the second component contains larger spectral density than

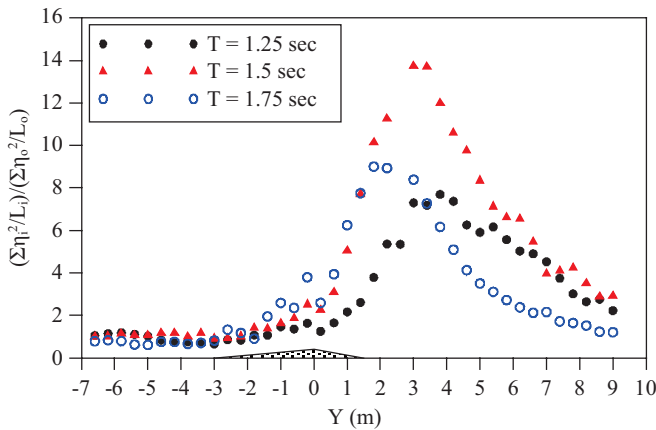


Fig. 11. Variations of wave energy ratio along the center line of the shoal for different wave period.

the principle component. The energies of third and fourth components are negligible. Fig. 10(c) shows the results for T = 1.75 sec case, the principle component for the spectra after the waves pass through the shoal contains the highest spectral density, but the second and third components both contain some non-negligible energy. The spectral densities of the first three components (principle, second, and third) are 3:2:1. The energies of fourth and fifth components are negligible.

The reason for wave energy behind the shoal being enlarged is due to combined effect of wave shoaling as the waves climb up to the crest line of the shoal, wave refractions at convex topography, and wave diffractions from two ends of the shoal induced by uneven bottom. The existence of multiple frequency components of waves behind the shoal is possibly related to the wave non-linearity induced by wave refraction and shoaling, and the interactions between highly non-linear waves from different directions and it needs further study.

From the point of view of wave energy concentration effect, Fig. 11 shows the energy ratio for the nodes along the center line of the shoal (at x = 0) from the front side to the back side. The wave energy enlarging ratio is defined as $(\sum \eta_i^2 / L_i) / (\sum \eta_o^2 / L_o)$, where $\sum \eta_i^2 / L_i$ and $\sum \eta_o^2 / L_o$ are respectively related to the wave energy per unit wave length at specific wave gauge and wave energy of incident waves, the subscript o denotes incident waves, $\eta_i(t)$ and $\eta_o(t)$ are the measured wave profiles, L_i and L_o are wave lengths. The section along the center line of the shoal is also illustrated on the bottom of the figure for reference. Before the incident waves reach the front end of the shoal, the ratio remains in unity with slightly energy loss which might be caused by the bottom friction. During the waves climb up to the top of the crest line, the energy ratio increased to around 2, 3, and 4 for the cases of T = 1.25 sec, 1.5 sec and 1.75 sec, respectively. After the waves pass through the top of the shoal, however, the energy ratio increases very rapidly. The maximum energy

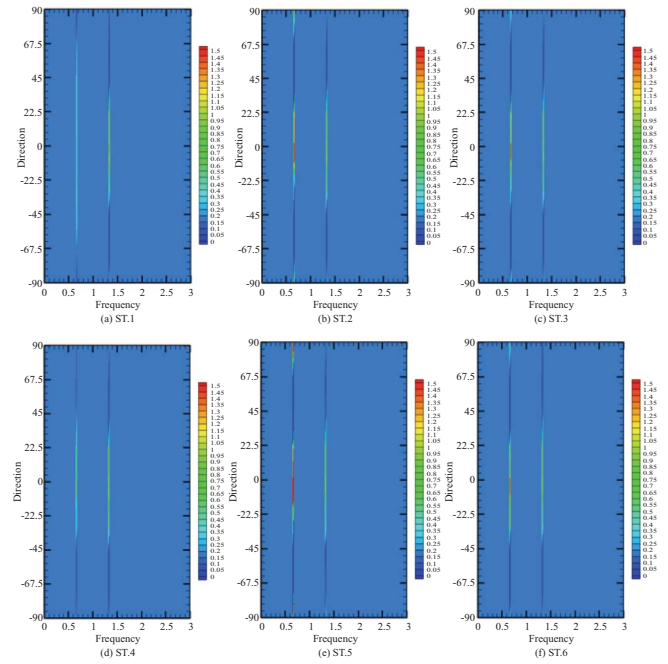


Fig. 12. Directional wave spectra at various locations (for T = 1.5 sec and $\theta_l = 0^\circ$ case).

ratio for the case of T = 1.25 sec is around 8 at y = 4.0 m; for the case of T = 1.5 sec is around 14 at y = 3.0 m; and for the case of T = 1.75 sec is around 9 at y = 2 m. Such phenomena demonstrate that the wave energy can be concentrated and enlarged by the new crescent shoal. The location of highest energy ratio occurs earlier in the long period wave cases. The energy ratio is not directly proportional to the wave period, however, the largest energy ratio occurs at the case of T = 1.5 sec. Due to the complexity of wave transformation around the shoal, such phenomenon should be an integrated result and cannot be explained easily. More detail studies should be done.

Although the experiments of this study adopts the unidirectional regular incident waves, the waves become multiply directional after they pass through the shoal due to the refraction and diffraction effects around the shoal. In order to investigate such a multiply directional wave field, a series of star array in accordance to the theory proposed by Borgman *et al.* in 1969 was deployed behind the shoal as shown in Fig. 6. Fig. 12 shows the directional wave spectra at ST.1 to ST.6 for the case of T = 1.5 sec and $\theta_l = 0^\circ$. The results show that multiple frequency component waves exist after the unidirectional regular waves pass through the crest line of the shoal. Such phenomena should be the reason that causes the wave heights behind the shoal varying alternatively high and low.

For the principle component, the wave energy directional spreading angle, with respect to the incident wave direction, is within $\pm 67.5^\circ$ at ST.1, $\pm 26^\circ$ at ST.2, $\pm 31^\circ$ at ST.3, $\pm 45^\circ$ at ST.4, $\pm 26^\circ$ at ST.5, and $\pm 33^\circ$ at ST.6. For the second com-

ponent, the wave spreading angle is all around $\pm 36^\circ$ for all six locations. The variations of the spreading angle of principle component should be related to the difference of the wave superposition of refraction waves and diffraction waves with different wave directions, wave heights and relative wave phases at different locations. The concentration of wave energy appears in the group type. Larger wave energies at ST.2 and ST.5, but for the rest of wave stations, the energy concentrations are not so strong. At ST.7, where the results are not shown in this paper, the multiple frequency components disappeared and only the principle component survived. Due to the spreading angles for second component at different wave stations are all around $\pm 36^\circ$, one can make a judgment that such component waves should be induced by a single source, and the most probable source is the waves passing through the top of the crest line of the shoal. When wave traveling from the front side to the back side of the shoal, the shoaling effect will enhance and strengthen the non-linearity of wave and thus cause the multiple frequency components.

V. CONCLUSIONS

This study focuses on the evaluation of wave energy concentration effect for regular waves passing through a new crescent type shoal seated on constant slope bottom. By using hydraulic model tests on a wave basin, the wave transformations and wave energy distributions under different incident regular wave periods were evaluated. From the discussions and comparisons, some conclusions are reached as the followings.

1. The crescent type shoal can concentrate wave energy and enlarge energy density behind the shoal. All the experimental results in this study indicate wave energy ratio above 8 times of the incident wave energy can be obtained for incoming wave passing through the shoal, especially for the case of wave period $T = 1.5$ sec this ratio reaches to 14 times.
2. The wave energy concentrating region locates behind the shoal which is radiated from the crescent shoal center, and major energy concentration region always locates along the direction of incoming wave. Furthermore, the location of the highest energy ratio for the major energy concentration region occurs closer to the shoal for the longer period incident wave is used.
3. The multiple frequency component waves occur behind the shoal is due to the wave superposition of the wave directly passing through the top of the shoal with strong non-linearity and refraction waves and diffraction waves with different wave directions.
4. The spreading angles of principle component of wave en-

ergy vary from location to location behind the shoal, and the spreading angle of energy for the second component is comparatively stable. For the case of $T = 1.5$ sec, the wave spreading angles of second component are all around $\pm 36^\circ$ for all six locations.

REFERENCES

1. Berkhoff, J. C. W., "Computation of combined refraction-diffraction," *Proceedings of 13th International Conference on Coastal Engineering*, Vancouver, ASCE, Vol. 1, pp. 471-490 (1972).
2. Berkhoff, J. C. W., Booij, N., and Radder, A. C., "Verification of numerical wave propagation models for simple harmonic linear water waves," *Coastal Engineering*, Vol. 6, pp. 255-279 (1982).
3. Borgman, L. E., "Directional spectral model for design use for surface waves," *Technical Report HELL 1-12, Hydraulic Engineering Laboratory*, University of California (1969).
4. Ebersole, B. A., "Refraction-diffraction model for linear water waves," *Journal of Waterway, Port, Coastal and Ocean Engineering*, Vol. 111, pp. 939-953 (1985).
5. Electric Power Research Institute (EPRI), *Oregon Offshore Wave Power Demonstration Project – Bridging the Gap Between the Completed Phase 1 Project Definition Study and the next Phase – Phase 2 Detailed Design and Permitting*, Report, 75 pages (2007).
6. Hsu, T. W., Tsay, T. K., Yen, C. C., and Chen, B. S., "Using finite element method to simulate nearshore wave field," *Proceedings of 20th Ocean Engineering Conference*, pp. 491-499 (1998).
7. Huang, I. C., *Experimental Study of Irregular Wave Propagating over an Elliptic Shoal on a Sloping Bottom*, Master Thesis, Department of Harbor and River Engineering, National Taiwan Ocean University (2007).
8. Imai, K., Akiyama, Y., Kudo, K., and Tsuzuku, T., "Study on wave force characteristic by a crescent submerged plate," *Proceedings of 35th Coastal Engineering Symposium*, pp. 522-526 (1988).
9. Imai, K., Akiyama, Y., Kudo, K., and Tsuzuku, T., "The wave focusing characteristic of the crescent submerged plate in varying directional wave field and the wave energy focusing utilization - the absorbing cell principle," *Japan Marine Engineering Essays*, Vol. 36, pp. 534-538 (1989).
10. Imai, K., Akiyama, Y., and Miami, S., "The wave focusing characteristic of the crescent submerged plate in varying directional wave field," *Japan Marine Engineering Essays*, Vol. 39, pp. 541-545 (1992).
11. Kirby, J. T. and Dalrymple, R. A., "Verification of a parabolic equation for propagation of weakly-nonlinear waves," *Coastal Engineering*, Vol. 8, pp. 219-232 (1984).
12. Kudo, K., Imai, K., Ikeya, T., Tsuzuku, T., and Akiyama, Y., "Study on wave focusing by a horizontally submerged plate," *Journal of the Society of Naval Architects of Japan*, No. 162, pp. 267-275 (1987).
13. Kudo, K., Tsuzuku, T., Akiyama, Y., and Imai, K., "Study on wave focusing by a horizontally submerged plate," *Journal of the Society of Naval Architects of Japan*, No. 160, pp. 217-225 (1986).
14. Mei, C. C., "Hydrodynamic principles of wave power extraction," *Philosophical Transactions of the Royal Society A*, Vol. 370, pp. 208-234 (2012).
15. Panchang, V. G., Cushman-Roisin, B., and Pearce, B. R., "Combined refraction-diffraction of short-waves in large coastal regions," *Coastal Engineering*, Vol. 12, pp. 133-156 (1988).
16. Wu, S. M., *Experimental Study of Regular Wave Propagating over an Elliptic Shoal On a Slope*, Master Thesis, Department of Harbor and River Engineering, National Taiwan Ocean University (2006). (in Chinese)